CHARACTERISTIC CRACK TIP FIELD AND THE CHARACTERIZING PARAMETERS FOR ELASTIC-PLASTIC FRACTURE MECHANICS

H. W. Liu and Tao Zhuang*

Department of Chemical Engineering and Materials Science, Syracuse University, Syracuse, NY 13210, USA

ABSTRACT

The linear elastic fracture mechanics can be formulated from the concept of a characteristic crack tip field, which is directly correlated with a well defined.fracture initiation process. This formulation is extended to the elastic-plastic fracture mechanics.

The stresses and strains at a crack tip are in a complicated three-dimensional state. There are three two-dimensional models of elastic-plastic crack tip fields: plane strain, plane stress, and strip yielding. The essential features of the crack tip fields of these three limiting cases are reviewed and analyzed, and the characterizing parameters for these three models are enumerated and their application to elastic-plastic fracture mechanics is discussed.

KEYWORDS

Crack tip field, characterizing parameters, elastic-plastic fracture mechanics.

INTRODUCTION

Griffith (1920) formulated the global energy balance fracture criterion for brittle solids from Inglis's (1913) elastic analysis of a stressed plate with an elliptical hole. As the minor axis approaches zero, the ellipse becomes a crack. The elastic crack tip field for a mode I opening crack can be written as (Williams 1957; Irwin 1957)

$$[\sigma_{ij},\varepsilon_{ij}] = \frac{K_I}{\sqrt{2\pi r}} [\tilde{\sigma}_{ij}(\theta),\tilde{\varepsilon}_{ij}(\theta)] \tag{1a}$$

$$u_i = \frac{K_I}{\mu}\sqrt{\frac{r}{2\pi}}\,\tilde{u}_i\,(\theta) \tag{1b}$$

μ is shear modulus.

*Central Iron and Steel Research Institute
Ministry of Metallurgical Industry, China

where r and θ are polar coordinates with the origin at the crack tip and the crack lying along the line θ = π. The terms $\tilde{\sigma}_{ij}(\theta)$, $\tilde{\varepsilon}_{ij}(\theta)$, and $\tilde{u}_i(\theta)$ define the θ-distributions of the corresponding stress, strain, and displacement components. K_I is the mode I stress intensity factor, which defines the entire crack tip stress, strain, and displacement fields. Therefore, one may say that K explicitly characterizes the elastic crack tip field.

K_I is related to the potential energy flux per unit area of crack extension, G_I.

$$G_I = \frac{K_I^2}{\bar{E}} \tag{2}$$

where $\bar{E} = E/(1 - \nu)$ for the plane strain case, and $\bar{E} = E$ for the plane stress case. If the surface energy is the only dissipative energy during crack propagation, G_{Ic} at fracture initiation must be equal to 2γ, where γ is surface energy per unit of crack area, and G_{Ic} at fracture initiation is a constant. Since G and K are related, K_{Ic} at fracture initiation must also be a constant.

For ideally brittle materials, the same conclusion that K_{Ic} = constant can be derived from the fact that K characterizes the elastic stresses and strains at a crack tip and the assumption that the same fracture initiation process will occur at the same crack tip field.

For metallic materials, plastic deformation will take place at the highly stressed region near a crack tip. The concept of a characteristic crack tip field (CCTF) which is directly correlated with a fracture initiation process in an elastic-plastic material as the fundamental basis of the linear elastic fracture mechanics, was suggested by Liu (1965,1966,1972) and was reviewed recently by Liu, Hu, and Kuo (1983).

The elastic crack tip field, Eqn. (1), is valid in a region r_e adjacent to a crack tip. If the applied stress is low enough, plastic deformation will occur only in a small plastic zone r_p, which is imbedded within the much larger elastic characteristic crack tip field zone r_e, Fig. 1. When $r_p << r_e$, the stress relaxation within r_p will not disturb the stresses on the boundary of r_e as given by the elastic solution, Eqn. (1). If $r_p << r_e$, the stress intensity factor K alone will be able to characterize the crack tip field even within r_p, and the crack tip field is invariant with in-plane geometric variations. This can be understood easily if one considers the region enclosed by r_e as a free body. On the boundary of the free body, the boundary stresses or displacements given by Eqn. (1) are imposed. Now let us consider the specimens with different in-plane geometries but loaded to the same K-value. The free bodies of all of the crack tip regions enclosed by r_e's are of the same size with the same boundary excitation. The crack tip stresses, strains, and displacements in these free bodies, even within r_p's must be the same for all of these specimens. Therefore, K characterizes the crack tip stresses and strains even within r_p. But the exact stresses and strains within r_p are unknown. Therefore we may say that K implicitly characterizes the crack tip field. Since these specimens have the identical crack tip field, if one specimen fractures, so will the others. This deduction leads us to conclude that K_c = constant.

The condition of $r_p << r_e$ is a sufficient condition for the validity of the linear elastic fracture mechanics (LEFM). In principle, this condition can always be satisfied by using a large enough specimen, since r_e is linearly proportional to specimen size. However, this condition is unduly severe in terms of specimen size requirements. The necessary condition for the validity of the LEFM is that K be able to characterize the crack tip stress or

strain component responsible for the defined fracture initiation process. The necessary condition for the plane stress case has been studied by Hu (1976) and Liu, Hu, and Kuo (1983).

The shortcomings of the global energy balance fracture criterion and the sharp notch theory as applied to the LEFM have been examined recently by Liu, Hu and Kuo (1983). The CCTF criterion for fracture initiation demands the identical crack tip field for a defined fracture initiation process in specimens of different geometries and is, therefore, much more severe than the global energy balance criterion.

To use the concept of CCTF for fracture analyses, the crack tip field must be well defined and thoroughly understood. Most of the theoretical analyses of crack tip fields are two-dimensional. There are three two-dimensional limiting cases: plane strain, plane stress, and Dugdale's strip yielding case. In this paper, the physical nature of the three limiting cases will be discussed; their characteristic crack tip fields will be reviewed; and the physical parameters that can be used to characterize these crack tip fields will be examined.

CHARACTERISTIC CRACK TIP FIELD AS A FRACTURE CRITERION

The concept of a critical CCTF for fracture initiation is applicable if the crack tip field can be written as the product of two factors, the crack tip field intensity I, and the crack tip field distribution function D:

$$\begin{aligned} \sigma_{ij} &= I(\text{geometry, loading}) \times D(r,\theta) \\ \varepsilon_{ij} &= I' \times D' \end{aligned} \tag{3}$$

where I and I' are functions of specimen geometry and loading. D and D' are invariants with in-plane geometric variations. Identical crack tip fields can take place in specimens of different geometry simply by adjusting the applied load. The linear elastic crack tip stress field, Eqn. (1), certainly fulfills this requirement. For the linear elastic case, D and D' can be written as $r^{\beta}\phi_{ij}(\theta)$, where $\beta = -1/2$, and ϕ_{ij} is a function of θ.

For a nonlinear solid obeying the pure power hardening relation, $\varepsilon/\varepsilon_o = \alpha(\sigma/\sigma_o)^N$, the crack tip field is (Hutchinson 1968; Rice and Rosengren 1968)

$$[\sigma_{ij},\sigma_e] = \sigma_o\left[\frac{J}{\alpha\sigma_o\varepsilon_o I_N r}\right]^{\frac{1}{N+1}} [\tilde{\sigma}_{ij}(\sigma,N),\sigma_e(\theta,N)] \tag{4}$$

$$\varepsilon_{ij} = \alpha\varepsilon_o\left[\frac{J}{\alpha\sigma_o\varepsilon_o I_N r}\right]^{\frac{N}{N+1}} \tilde{\varepsilon}_{ij}(\theta,N) \tag{5}$$

$$u_i = \alpha\varepsilon_o\left[\frac{J}{\alpha\sigma_o\varepsilon_o I_N}\right]^{\frac{N}{N+1}} r^{\frac{1}{N+1}} \tilde{u}_i(\theta,N) \tag{6}$$

In these equations, J is identified with the intensity. The crack tip field is the product of a function of J and the distribution function D. β and β' are 1/(1+N) and N/(1+N) respectively. If $\tilde{\sigma}_{ij}$, $\tilde{\varepsilon}_{ij}$, and $\tilde{u}_i$ are invariant to in-plane geometric variations, the crack tip field given by Eqns. (4), (5), and (6) can serve as the CCTF. If (4,5,6) are valid, the same crack tip field can be obtained in any specimen geometry simply by adjusting the applied load and J. Therefore, the crack tip field for a material obeying the pure power hardening relation fulfills the requirement stated in Eqn. (3). These results , Eqns. (1a), (1b), (4), (5), (6) suggest that the distribution function of a crack tip field is dominated by the complete and sharp re-entrant angle geometry of the crack. Its independence from the in-plane geometric variations, perhaps, is not limited to elastic and pure power hardening materials. However, its generality needs to be explored.

If a CCTF exists, the extension of the LEFM to elastic-plastic fracture mechanics becomes simple. Fracture initiation takes place when a brittle particle or embrittled grain boundary is broken or when shear slip takes place at a crack tip. These local fractures and slips at a crack tip are caused by the crack tip stresses and strains. It is expected that identical crack tip stresses and strains should induce identical material responses, i.e., either local fracture or local slip identified with the fracture initiation process, provided the size of the CCTF is large enough to cover the fracture processing zone (Liu, 1983). The advantage of using CCTF is that the criterion is applicable to any micrometallurgical fracture initiation process as long as the process is caused by crack tip stresses and strains.

The concept of a characteristic state of stresses and strains to signify a specific material response is well accepted. For example, the yield strength of a polycrystal signifies the beginning of a large-scale dislocation motion. For a single crystal, a dislocation starts to move when the resolved shear stress reaches a critical value. The yield strength and the critical resolved shear stress characterize implicitly the state of the stresses at the core of the dislocation, where the interatomic bond is overcome and the atoms on two opposing sides of the slip plane slip over each other. The interatomic bond in shear is on the order of magnitude of $\mu/10$, where μ is the shear modulus. Therefore, the yield strength and the critical resolved shear stress characterize the state of stress at the core of a dislocation that is tens or even hundreds of times greater than the applied stresses.

Fracture in a high-strength material is often initiated at brittle inclusions or precipitates or at embrittled grain boundaries or particle-matrix interfaces. Once the fracture is initiated at these sites, fracture can proceed by the mechanism of plastic deformation. The processes of void initiation and void growth have been the subjects of many studies (McClintock, 1968; Argon, 1976). At the sites of local fracture initiation and fracture propagation, the applied stress is magnified many times by dislocation arrays and geometric and metallurgical notches. Therefore, the applied "fracture stress" that implicitly characterizes the local stress at the site of fracture initiation and propagation many times greater, are often in the neighborhood of E/10. To break the interatomic bond either by shear separation or by normal separation, a local stress on the order of magnitude of $\mu/10$ or E/10 is necessary. The yield strength, the critical resolved shear stress, and "fracture" stress characterize such states of local stresses.

One necessary condition to be able to characterize the local stress is that it must bear a definite relation to the applied stress. However, the relation may remain unknown, i.e. implicit characterization. If a definitive relation is lacking, the principle of characterization fails.

Stresses and strains at a crack tip are complex and three-dimensional. The majority of the crack tip field analyses are two-dimensional. Only these two-dimensional models are understood well enough to establish the characteristic field analysis. There are three two-dimensional limiting cases: plane strain, plane stress and strip necking cases, which can be adapted for elastic-plastic fracture mechanics study.

The crack tip field in a small region in the vicinity of a crack tip and in the interior of a thick specimen is in the state of plane strain. On the specimen surface, the state of stress is plane-stress. The plane stress plastic zone on the surface is larger than the plane strain plastic zone in the interior as shown schematically in Fig. 2. A transition region exists between the plane-stress plastic zone on the surface and plane-strain plastic zone in the interior. The state of plane strain is induced by the steep strain gradient $\partial(\varepsilon_{11}+\varepsilon_{22})/\partial x_i$ and by the constraint from thickness contraction by the bulk material farther away from the crack tip. In the region far away from the crack tip, the strain gradient is low, and the state of stress is plane-stress. A transition region also exists between the two regions.

Figure 3 compares the measured strain ε_{yy} in an aluminum specimen with the finite element calculation (Hu and Liu, 1976). The specimen was in deep general yielding. The strains were measured on the specimen surface by the moire method. The measurements agree well with the plane stress calculations (solid lines) except in a small region in which r<t, where t is plate thickness. Within this small region, the thickness constraint induces a triaxial state of stresses in the interior, reduces the deviatoric stresses, and "stiffens" the deformation resistance of the material. This decrease in plastic deformation is reflected in the surface strain measurements. The experimental results indicate that the size of the stiffened region is equal to the plate thickness (Hu and Liu, 1976; Liu and Ke, 1975). The measurements and the plane-stress FEM calculations agree well with the HRR crack tip field.

When crack tip plastic deformation is extensive, crack tip necking takes place. Figure 4 shows the moire fringe picture of a crack tip necking zone. The y-displacement along each fringe is constant, and the strain ε_{yy} is inversely proportional to the fringe spacing in the y-direction. There is a sharp bend in each of the fringes originating at the crack tip. Within the region defined by the sharp bends, the y-fringe spacings are much smaller than those outside of the region. This is a region of much higher strains. The transition from low-strain to high-strain regions is abrupt, suggesting a discontinuity in strain gradients across the necking boundary.

When plastic deformation is extensive and when the plate is very thin, a strip necking zone will occur as shown clearly in a thin steel specimen in Fig. 5. In summary, (1) the plane-strain case exists in a small region near the crack tip if a plate is very thick relative to the plastic zone size. The bulk of a specimen is in the state of plane stress. (2) The plane-stress case is applicable to the bulk of a sample, if the size of the plane stress CCTF is several times the plate thickness. However in the crack tip stiffened zone, the stresses and strains are three-dimensional. It is within this region that fracture is initiated. (3) The strip yield model is applicable if the crack tip plastic zone is many times the plate thickness. For the strip yielding model, the stresses and strains near the crack tip in a strip necking zone are three-dimensional. Again fracture initiation occurs in the region of three-dimensional stresses and strains. If the three-dimensional stresses, strains, and displacements can be characterized by the mechanical parameters of the three two-dimensional models, these models can be used for fracture analyses by using the concept of CCTF.

Characteristic Crack Tip Fields and Their Characterizing Parameters

The crack tip field derived by Hutchinson (1968) and Rice and Rosengren (1968), Eqns. (4,5,6) are asymptotic solutions valid in a region close enough to a crack tip. Furthermore, the validity of these equations might be subjected to limitations of specimen size and level of loading. Therefore, it is prudent to analyze the details of the crack tip field before it is applied to fracture analysis.

The plane stress crack tip fields in double-edge-cracked plate and single-edge-cracked plate in tension have been calculated by the finite element method (Hu, 1976; Hu, Kuo and Liu, 1975; Hu and Liu, 1976). They have shown that an unique correspondence exists between the crack tip field in these specimens in general yielding, GY, and the crack tip field in small-scale yielding, SSY. In other words plane stress crack tip field in a small sample in GY corresponds directly with the crack tip field in a large specimen in SSY. One would be able to obtain the equivalent K-value of a small specimen in GY from the correspondence with the large specimen in SSY. The value of J is directly related to that of K. Therefore, the J-value can also be found by the correspondence. It was also found that the plane stress crack tip field calculated by the FEM, σ_{yy}, ε_{yy}, $\bar{\sigma}$, and $\bar{\varepsilon}_p$ agrees well with the HRR crack tip field.

However, in both double-edge-cracked and single-edge-cracked specimens in tension, the bending moment is zero or very close to zero. The bending itself may introduce stress and strain gradients. The added bending gradient may disturb the crack tip field given by Eqns. (4,5,6). Furthermore, Eqns. (4,5,6) were derived for pure power hardening materials. The stress-strain relations of real materials are better represented by the Ramberg Osgood relation or by the piecewise power hardening relation. Therefore, it is desirable to verify the existence of a characteristic plane stress crack tip field for such σ-ε relation for double-edge-cracked, DEC; single-edge-cracked, SEC; and center-cracked planes, CCP, in tension and three-point bending specimen, TPB. The first three specimen types have no bending or very little bending. The DEC and CCP are subjected to uniform boundary displacement. SEC is subjected to a concentrated tensile load. Piecewise power hardening relation was used.

$$\begin{aligned} \sigma &= E\varepsilon && \sigma \leq \sigma_Y \\ (\sigma/\sigma_Y) &= (\varepsilon/\varepsilon_Y)^n && \sigma > \sigma_Y \end{aligned} \qquad (7)$$

$\sigma_Y = 0.56\ KN/mm^2$; strain hardening exponent $n = 0.11$; Young's modulus $E = 200\ KN/mm^2$; and Poisson's ratio $\nu = 0.3$. The ABAQUS-version III finite element computer program was used. The typical finite element mesh involves 136 elements and 465 node points. Eight wedge-shaped degenerated eight-noded isoparametric elements are employed. The crack tip is degenerated with 17 nodes, which are allowed to displace independently from each other. The radial length of the elements closest to crack tip, is 1/1000 of the ligament size. Prandtl-Reuss flow rule and small strain formulations were used. About 200 increments are employed to cover the range from the small scale yielding to the deep general yielding.

Figure 6 shows the plot of σ_{yy} and ε_{yy} along the crack line of the three-point bend specimen. In the log-log plot, all the lines for σ_{yy} have the same slope, as do the lines for ε_{yy}. Figure 7 shows the same data in the log (σ_{yy}/σ_Y) vs. log (r/r_p) plot; where σ_Y is the tensile yield stress, and r_p is the plastic zone size. The value of r_p is obtained by extrapolating the curve of log $\bar{\sigma}$ vs. log r to the location where $\bar{\sigma} = \sigma_Y$. The top curve in Fig. 7 is still in the state of SSY, where r_p is only 1/20

of the ligament size. In Fig. 7, the ε_{yy} data are also shown. As the load increases, the stress and strain curves bend down and deviate from that of the SSY. This is caused by the gradient due to the bending across the ligament of the specimen. However, it is clear from the data in Fig. 6 that the absolute size of the characteristic crack tip field increases with the applied load. The curve at the higher load is contracted to the left because of the large size of the extrapolated r_p used to normalize the plot. The extrapolated value of r_p at the highest load level in Fig. 7 is 100 to 300 times the value of r_p at the lowest load level. These results indicate that the stress field due to bending does not impose serious limitations on the size of the plane stress test specimens.

Similar plots for double-edge-cracked, single-edge-cracked, and center-cracked specimens in tension are also shown. The effect of bending on the CCTF is most severe in the three-point bend specimen. However, even in this case, the effect of bending is not significant enough to impair the applicability of the CCTF for fracture analysis. In Fig. 8, the portions of the stress and strain data within the characteristic crack tip field are plotted together for all four types of specimens. The curves of all four types of specimens coincide with each other. The data clearly indicate that a plane-stress CCTF exists for all four major types of specimen geometry. The slopes of the $\bar{\sigma}$ and $\bar{\varepsilon}_p$ curves are 0.09 and 0.89. The sum is 0.98 which agrees well with the values given by HRR theory.

The crack tip stiffened zone is imbedded in the characteristic crack tip plane-stress zone as shown by the moire strain measurements, Fig. 3 (Hu 1976, Hu, Kuo, and Liu 1975, and Hu and Liu 1976). The fracture initiation process takes place within the stiffened zone, where the precise stresses and strains are unknown but are implicitly characterized by K or J, if the size of the characteristic plane stress zone is much larger than the stiffened zone.

On the other hand, the crack tip field given by Eqns. (4,5,6) is not universally valid in the plane-strain case. McMeeking and Parks (1979) and Shih and German (1981) studied the characteristic crack tip fields in large-scale yielding, LSY, and in GY. In McMeeking and Parks's calculation, the large deformation theory was used. Figure 9 shows the plot of σ_{yy}/σ_o vs. $r/(J/\sigma_o)$ along the crack line in a central cracked panel in tension. The data of SSY as well as LSY and GY are plotted. The quantity σ_{yy}/σ_o at the higher loads is considerably lower than that of SSY. This deviation imposes a specimen size limitation. The results of McMeeking and Parks and Shih and German indicate that the crack tip fields agree with the HRR field when the ligament exceeds 25 to 50 times J/σ_{flow} for the cracked bend specimen and the compact tension specimen, and the relevant dimensions must exceed 200 times J/σ_{flow} for center-cracked panels in tension. When a specimen is too small, the CCTF is not well developed. If the CCTF is not well developed, the stresses and strains at the site of fracture initiation may vary from one specimen to another even though the imposed J-value is the same. Therefore it is expected that J_c or δ_c will not be a geometric invariant quantity as shown by the measurements of Hancock and Cowling (1980). Therefore J is applicable for fracture toughness evaluation only if a CCTF exists; and, it is not applicable if a CCTF is lacking.

In the plane strain case, a universally valid crack tip field is lacking. Therefore it is necessary to choose a reference to serve as the CCTF. Since the crack tip field in SSY is unique, it is the natural choice.

For the plane stress case, the near tip field is related to the far field parameters; the applied stress σ_∞ and the applied strain ε_∞. For small strain deformation theory, incompressible solids conforming to the pure power hardening stress-strain relation under a proportional loading,

Ilyushin (1947) has shown that if the boundary traction increases linearly in proportion to a single load parameter P, the stresses at each point in the solid also vary linearly with P. In other words, the near tip stresses and strains will be proportional to the applied stress σ_∞ and the applied strain ε_∞. Equations (4,5,6) indicate that J is proportional to the product of a near tip stress component and its corresponding strain component, which in turn, according to Iluyshin, should be proportional to the product $(\sigma_\infty\varepsilon_\infty)$. Of course, this relation is subject to the limitations imposed by the assumptions by Iluyshin and Hutchinson and Rice and Rosengren in their derivations. For a piecewise power hardening material, Hu (1976) and Liu, Hu and Kuo (1983) have demonstrated that the linear relation between J and $\sigma_\infty\varepsilon_\infty$ indeed exists for the plane stress case. For the plane strains case, a similar relation exists, but its applicability is complicated by the transition from the near tip plane-strain region to the far field plane-stress region.

The extent of crack tip necking increases with plastic zone size. The ratio r_p/t gives a measure of necking tendency. As the ratio $\eta = (K/\sigma_Y)^2/t$ increases, crack tip deformation approaches that of strip yielding model. Figure(10)shows the measured and calculated crack opening displacements in aluminum specimens. The measured opening displacements and the strip yielding model calculations agree very well if $\eta = 18$. The measured displacements agree well with the elastic calculations when $\eta = 1$. When plastic zone is much larger than thickness, crack tip deformation becomes that of strip yielding model. Figure(11) compares the measured opening displacements and the strip yielding calculations along the crack surface as well as in the strip necking zone in a thin steel specimen. The agreement is very good. For this specimen, ratio $\eta = (K/\sigma_Y)^2/t$ is equal to 48. Furthermore, within the strip necking zone, the opening displacements agree well with the thickness contraction (Schaeffer, Ke and Liu, 1971).

Within the strip necking zone, the deformation is three-dimensional, especially the stresses and strains close to the crack tip. The y-displacements (v) along a line perpendicular to the crack plane at a distance x from the crack tip were measured. The measurements were made on both sides of the crack line along three different straight lines at three different distances from the crack tip. The measurements are plotted in the (v/t) vs. (y/t) diagram in Fig. (12). Measurements from two specimens of different thicknesses were made. For the data in Fig.(12), the sizes of the necking zones r_N, are proportional to their specimen thicknesses, t. The locations of the straight lines were so chosen that $r_{N(thick)}/r_{N(thin)} = t_{(thick)}/t_{(thin)} = x_{(thick)}/x_{(thin)}$. The data from these two specimens lie on top of each other. This suggests that the three-dimensional state of stresses and strains at the crack tip of a strip necking zone can be characterized by the ratio of crack tip opening displacement to plate thickness, δ_o/t; and the crack tip field might be written in the form $(\delta_o/t)f(r/t)$.

The stress, strain, and displacement components of the crack tip field and K and J are interrelated for power hardening elastic-plastic solids in plane stress. If any one of the stress, strain, or displacement components is known, the entire crack tip field is defined. In principle, any one of these components as well as K and J can be used to characterize the entire crack tip field, provided the size of the plane stress CCTF is several times the plate thickness. Figures (3,6,7 and 8). However, near tip stress, near tip strain, crack opening displacement at a small distance from the tip, K and J are more meaningful and practical. As crack tip plastic deformation increases and η reaches the value of 18, crack tip opening displacement at a small distance from a crack tip can be used to characterize the crack tip field, Fig.(10). As crack tip plastic deformation is further increased to

$\eta = 48$, crack opening displacement, crack tip opening displacement (Fig. 11 and 12) and thickness contraction (Schaeffer, Ke, and Liu 1971; and Liu and Kuo, 1979) are able to characterize the crack tip field. Figure 13 shows various regions, where these three two-dimensional models are applicable and their characterizing parameters. Because of the lack of sufficient data, the demarcations are tentative.

SUMMARY

This paper has briefly reviewed the formulation of the characteristic crack tip field as the fundamental basis of the linear elastic fracture mechanics. The basic concept of correlating mechanical behaviors with their corresponding characteristic stresses and strains is discussed. The crack tip stresses and strains are complicated and three-dimensional. There are three two-dimensional limiting cases: plane strain, plane stress, and strip yielding. The characteristics of the crack tip fields in these three models are analyzed, and their application to elastic-plastic fracture mechanics is discussed. The promising characterizing parameters include K or J, near tip stress, near tip strain, crack tip opening displacement, crack opening displacement at a small distance from a crack tip, and thickness contraction along the fracture path.

ACKNOWLEDGMENT

The financial support by the Dept. of Chem. Eng. and Mat. Science of the Syracuse University and the visiting scholarship by the People's Republic of China to one of the authors, Tao Zhuang are gratefully acknowledged.

REFERENCES

Argon, A.S., Jan. (1976). J. Eng. Mats. and Tech., Trans of the ASME, 60-68.
Griffith, A.A. (1920). Phil. Trans. of the Royal Society (London) Series A 221, 163-198.
Hancock, J.W. and Cowling, M.J., Aug.-Sept. (1980). Metal Science, 293-304.
Hong, C.E. (1984) M.S. Thesis, Solid State Science and Technology, Syracuse University.
Hu, W.L. (1976) Ph.D. Dissertation, Solid State Science and Technology, Syracuse University.
Hu, W.L., Kuo, A.S. and Liu, H.W. (1975). A Study of Crack Tip Deformation and Ductile Fracture, Proc. 12th Annual Meeting of the Soc. of Eng. Sci., University of Texas.
Hu, W.L. and Liu, H.W. (1976). ASTM STP601, 522-534.
Hutchinson, J.W. (1968). J. Mech. and Phys. of Solids, 16, 13-31.
Ilyushin, A.A. (1946). The Theory of Small Elastic-Plastic Deformations, Prikadnaia Matematika i Mekhanika, P.M.M 10, 347.
Inglis, C.E. (1913). Trans. of Navel Architects (London) 60, 213.
Irwin, G.R. (1957). J. Applied Mech. 24, No. 3.
Liu, H.W. (1965). STP 381, ASTM, 23-26.
Liu, H.W. (1966). J. of Frac. Mech. 2, 393-399.
Liu, H.W. (1972). An Analysis on Fatigue Crack Propagation, NASA CR-2032.
Liu, H.W. (1983). J. Eng. Frac. Mech. 17, No. 5, 425-438.
Liu, H.W., Hu, W.L. and Kuo, A.S. (1983). ASTM Second Symposium Elastic-Plastic Fracture 2, 632.
Liu, H.W. and Ke, J.S. (1975). SESA Monograph on Experimental Technique on Fracture Mechanics 2, 111-165.
Liu, H.W. and Kuo, A.S. (1978). Int. J. of Fract. 14, R109-R112.
McClintock, F.A. (1968). J. Appl. Mech. 35, 363.
McMeeking, R.M. and Parks, D.M. (1979). ASTM STP668, 175-194.
Rice, J.R. and Rosengren, A.F. (1968). J. Mech. and Phys. of Solids 16, 1-12.
Schaeffer, B., Ke, J.S. and Liu, H.W. (1971). J. of Experim. Mech., April,1-4
Shih, C.F. and German, M.D. (1981) Inter. J. of Frac. 17, 1, 27-43.
Williams, M.L. (1957). J. of Appl. Mech. 24, 109-114.

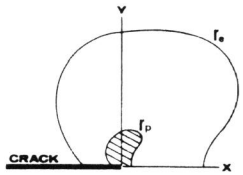

Fig. 1. A small plastic zone r_p is imbedded within the much larger CCTF field zone r_e at a low applied stress.

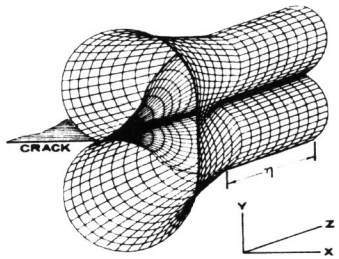

Fig. 2. Schematic diagram showing the crack tip plastic zone. Only half of the zone is shown. η is the fully developed plane strain zone. The double cone is the plane strain zone in the near surface layer. (Hu, Kuo, Liu 1975)

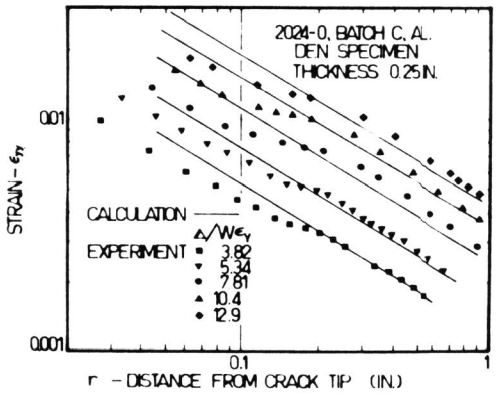

Fig. 3. Comparison of calculated and measured ϵ_{yy} for an aluminum specimen. Crack tip stiffening reduces strains in the near tip region. (Liu, Hu, Kuo 1983)

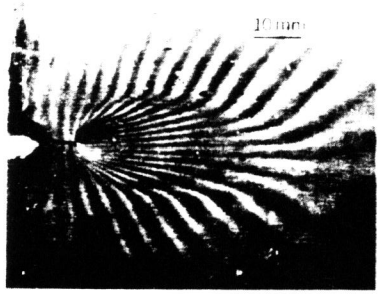

Fig. 4. A Moire fringe pattern showing crack tip necking. (Hong 1984)

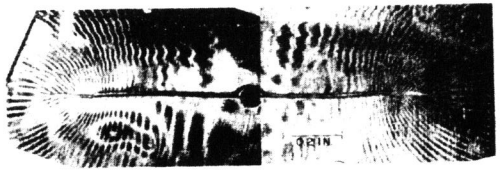

Fig. 5. Moire pattern of a steel specimen: applied stress, 55 ksi; 0.2-percent-offset yield stress, 91 ksi; Young's modulus, 32 x 10^6 psi; 0.012-in. thick; 6-in. wide; slot length, 1.0 in.; pitch of moire grille, 1/13,400 in. (Schaeffer, Ke, Liu 1971)

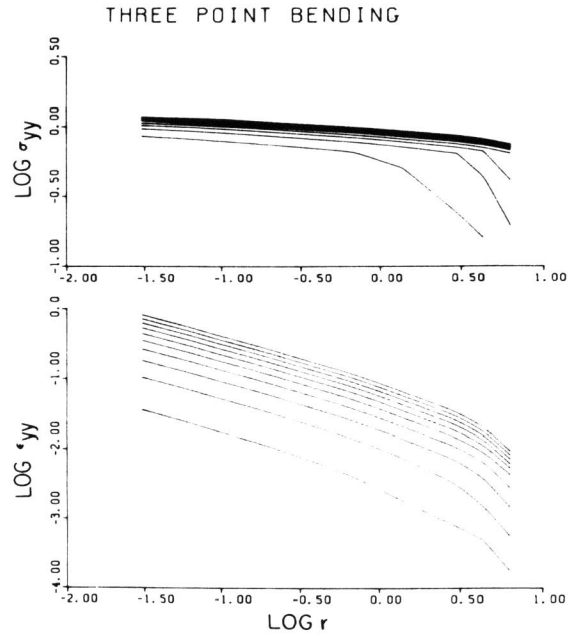

Fig. 6. Variations of σ_{yy} and ϵ_{yy} along crack line. From small scale yielding to deep general yielding.

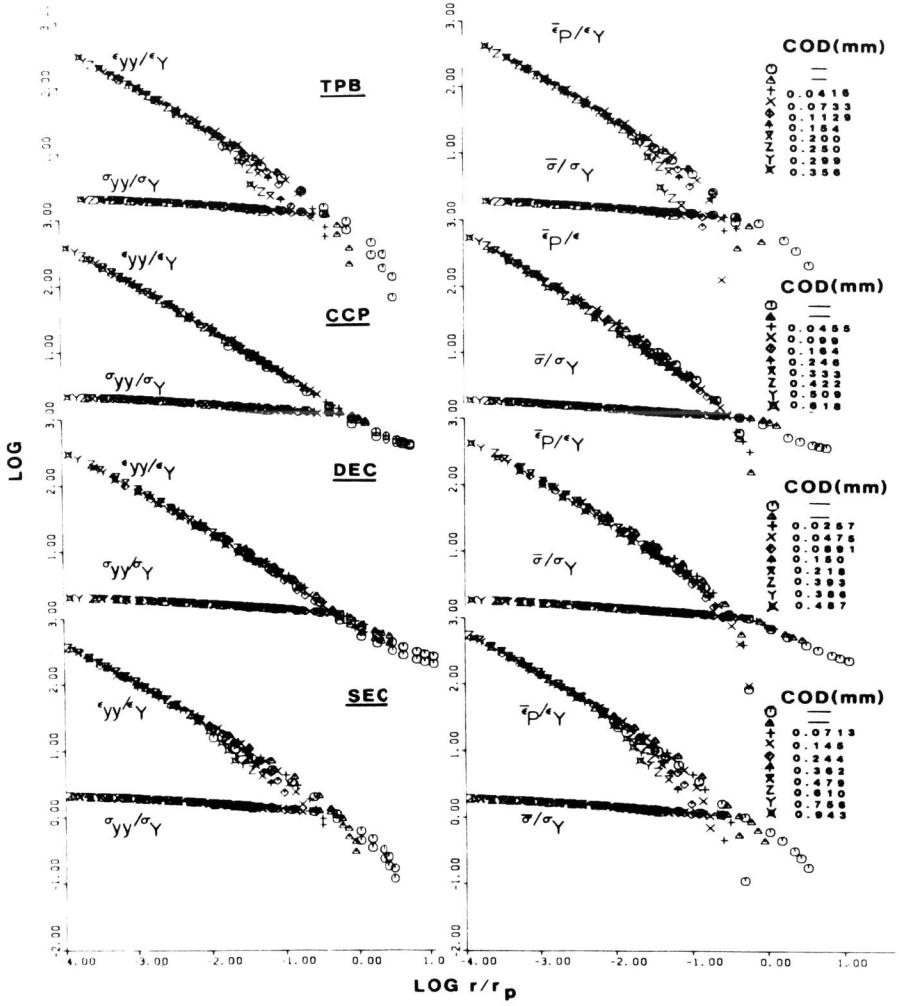

Fig. 7. Normalized σ_{yy}, ε_{yy}, $\bar{\sigma}$ and $\bar{\varepsilon}_p$ along crack line for TPB, CCP, DEN and SEN specimens, from small scale yielding to deep general yielding.

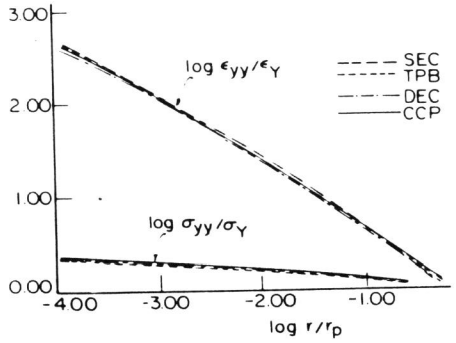

Fig. 8. Normalized σ_{yy} and ε_{yy} along crack line within characteristic crack tip field for all four types of specimens.

Fig. 9. Normal stress on plane ahead of crack tip vs. distance for center-cracked panel with a/w= 0.9 and N=0.1, Note that the maximum attained normal stress is decreasing at the large J value (McMeeking and Parks, ASTM STP668).

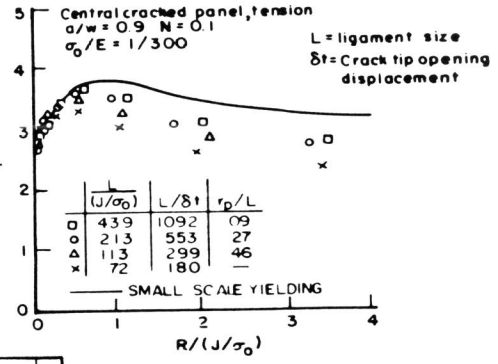

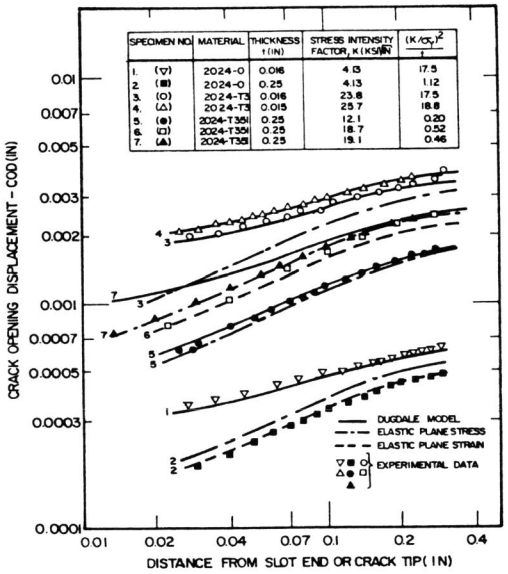

Fig. 10. Comparison of measured and calculated COD for aluminum specimens.
(Hu, Kuo, Liu 1975)

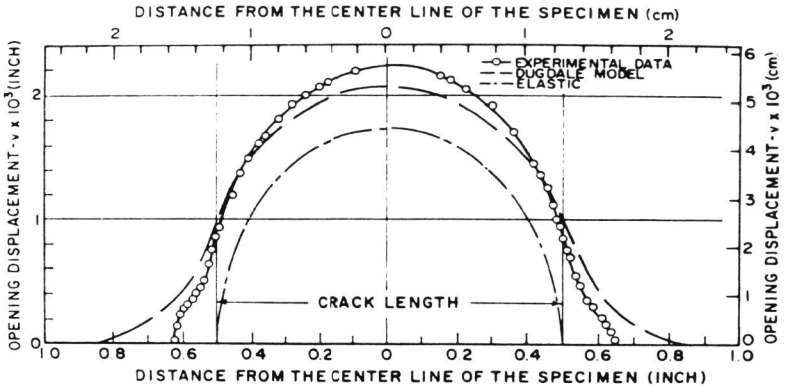

Fig. 11. Comparison of measured and calculated COD for a thin steel specimen with $(K/\sigma_Y)^2/t = 48$. (Schaeffer, Ke, and Liu, 1971)

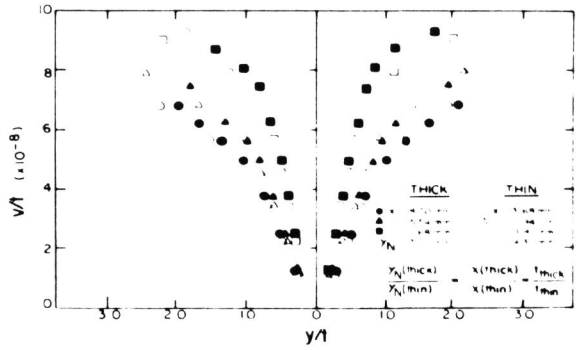

Fig. 12. Y-direction displacement field (v) normalized with specimen thickness (t) for thick and thin specimens. (Hong 1984)

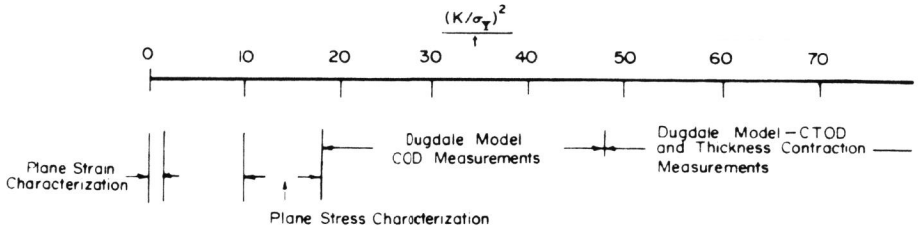

Fig. 13. Thickness effects on the choice of fracture criteria. (Liu, Hu, Kuo 1983)